Sirte University Scientific Journal Vol. 13, No. 1 (2023) 25-33

Sirte University Scientific Journal (SUSJ)

Journal home page: http://journal.su.edu.ly/index.php/SUSJ/index
DOI: 10.37375/ISSN:2518-5454

Modified Empirical Models for Predicting Liquid Film Thickness in Different-Sized Vertical Pipes

Almabrok A. Almabrok

Petroleum Engineering Department, Faculty of Engineering, Sirte University, Sirte, Libya.

DOI: https://doi.org/10.37375/susj.v13i1.1368

ARTICLE INFO:

Received 13 September 2022.
Accepted 10 January 2023.
Available online 01 June 2023.

Keywords: (*Liquid film Thickness, Gas-Liquid, Empirical Models, Large-Diameter*).

A B S T R A C T

The liquid film thickness is a vital parameter in many engineering applications such as production equipment of oil and gas. Good control of fluid flow in such equipment can lead to maintaining a continuous liquid film on the pipe wall and hence increasing the anticipated production rate and avoiding catastrophic consequences. Therefore, a precise estimation of liquid film behavior is required to achieve the targeted production rate and overcome the above-mentioned issues.

Even though a considerable number of empirical models were reported, most of these assessed the fluid flow based on small-sized pipes. These models incorrectly predicted the film thickness if applied to a large-diameter.

This work was aimed at developing correlations for gas-liquid two-phase fluid in order to be applicable for different-sized pipes. The new correlations were evaluated against a wide range of experimental data of liquid film and for different diameters collected from the literature on vertical pipes. It was found that the new correlations can be precisely used for predicting the liquid film behavior in small and large pipe diameters.

1 Introduction

A number of empirical models for predicting film thickness, interfacial shear stress, interfacial friction factor, and frictional pressure drop are correlated with the Reynolds number of the liquid film with dimensionless film thickness, as presented by the following formula:

$$\delta^+ = A\, Re_{Lf}^B \quad (1)$$

A and B are regression constants. Kosky (1971) had earlier determined A and B to be A=0.0512, B= 0.875 for Re_{Lf}>1000 and Asali et al. (1985) obtained A= 0.34 and B = 0.6 for $Re_{Lf} < 10^3$. More validated values are published by various authors for vertical air-water flow in pipes of varying diameters. These include Ambrosini et al. (1991) and Kaji & Azzopardi (2010).

The dimensionless film thickness δ^+ is defined analogously to y^+, and the friction distance parameter is:

$$\delta^+ = \frac{\delta}{\mu_L} U^* \quad (2)$$

The friction velocity (U^*) is defined as follows:

$$U^* = \sqrt{\frac{\tau_i}{\rho_L}} \quad (3)$$

The interfacial shear stress (τ_i) is given by:

$$\tau_i = \frac{1}{2} f_i \rho_g u_{sg}^2 \quad (4)$$

Where ρ_g and u_{sg} are, respectively, the gas density and its superficial velocity. Kaji & Azzopardi (2010) reported that the interfacial friction factor f_i is defined by correlations reported by Ambrosini et al., (1991) & Holt et al., (1999) and it depends on the mass flux of gas phase, $\dot{m}_g$:

$$\frac{f_i}{f_s} = 1 + 13.8 {We_D}^{0.2} Re_g^{-0.6} \left(\delta_g^+ - 200\sqrt{\frac{\rho_g}{\rho_L}}\right) \quad (5)$$

***Corresponding author*: E-mail: almabrok.abushanaf@su.edu.ly**

for $\dot{m}_g \leq$100 kg/m^{2}s

$$\frac{f_i}{f_s} = 1 + 13.8We_D{}^{0.175}Re_g^{-0.7} \quad (6)$$

for $\dot{m}_g >$100 kg/m^{2}s

Where:

$$\dot{m}_g 8 * 8 * /7888 = \tfrac{\pi}{4}\rho_g u_g \quad (7)$$

u_g is the gas core velocity which is defined as:

$$u_g = \frac{u_{sg}}{\alpha} \quad (8)$$

α being the void fraction estimated as $(D_t - 2\delta)/D_t$ assuming the liquid film is symmetrical and smooth with negligible entrainment only for the purpose of calculating u_g, Re_g, We_D, and f_s.

$$Re_g = \frac{\rho_g u_g D_t}{\mu_g} \quad (9)$$

$$We_D = \frac{\rho_g u_g^2 D_t}{\sigma} \quad (10)$$

$$\delta_g^+ = \frac{\delta \rho_g}{\mu_g}\sqrt{\frac{\tau_i}{\rho_g}} \quad (11)$$

$$f_s = 0.046Re_g^{-0.2} \quad (12)$$

σ, μ_g, and f_s are respectively, surface tension, the dynamic viscosity of the liquid phase, and the single-phase friction factor. If film thickness values are available experimentally, Equations (2)–(12) have to be solved iteratively for the interfacial friction factor, dimensionless film thickness, and interfacial shear stress. This is a variation of the triangular relationships described by Hewitt & Hall-Taylor (1970) and Hewitt & Govan (1990). With knowledge of the film velocity, the liquid film Reynolds number Re_{Lf} in Equation (1) can be obtained from:

$$Re_{Lf} = \frac{\dot{m}_{Lf} D_t}{\mu_L} \quad (13)$$

Where:

$\dot{m}_{Lf}$ is the mass flux of liquid film in kg/m^{2}s as a function of the film velocity (u_{Lf}) is described by the following equation:

$$\dot{m}_{Lf} = \frac{4\rho_L u_{Lf}\,\delta}{D_t} \quad (14)$$

This is only valid for low gas flow rates where there is negligible entrainment or for equilibrium flows where it can be assumed that the deposition rate cancels out the entrainment rate *E*. However, for thin films at high gas flow rates, liquid entrainment into the gas core can be significant and may have to be adjusted against the rate of deposition *D* in what is a non-equilibrium flow. This is done by carrying out a mass balance described by equation (15).

$$\frac{d\dot{m}_{Lf}}{dz} = \frac{4(D-E)}{D_t} \quad (15)$$

Where z is defined as the axial distance throughout the flow path. The equations for *D* and *E* (kg/m^{2}s) are as reported by Hewitt & Govan (1990). They noted that the major difficulty with Equation (15) is selecting the correct boundary conditions. This is tackled by assuming a zero flow rate of liquid film at the input section of the conduit or can be arbitrarily estimated for example by supposing a liquid phase fraction in the film of liquid at a known quality. The entrainment rate *E* is correlated using the:

$$\frac{E}{\dot{m}_g} = 5.75 \times 10^{-5}\left[\left(\dot{m}_{lf} - \dot{m}_{lfc}\right)^2 \frac{D_t \rho_L}{\sigma \rho_g^2}\right]^{0.316} \quad (16)$$

Where $\dot{m}_{lfc}$ is the critical liquid mass flux when entrainment begins and is calculated as follows:

$$\dot{m}_{lfc} = \frac{\mu_L}{D_t}\exp\left(5.8504 + 0.4249\frac{\mu_g}{\mu_L}\sqrt{\frac{\rho_L}{\rho_g}}\right) \quad (17)$$

The deposition rate *D* is defined by:

$$D = kC \quad (18)$$

The deposition mass transfer coefficient (k) is correlated as a function of surface tension σ:

$$k\sqrt{\frac{\rho_g D_t}{\sigma}} = 0.18 \text{ for } \frac{C}{\rho_g} \leq 0.3, \quad (19)$$

$$k\sqrt{\frac{\rho_g D_t}{\sigma}} = 0.083\left(\frac{C}{\rho_g}\right)^{-0.65} \text{ for } \frac{C}{\rho_g} > 0.3. \quad (20)$$

Henstock & Hanratty (1976) created the following model based on the experimental data of water and air for upflows.

$$\delta^+ = [\left(0.707Re_{Lf}^{0.5}\right)^{2.5} + \left(0.039Re_{Lf}^{0.9}\right)^{2.5}]^{0.4} \quad (21)$$

They calculated δ^+ using a method for estimating the interfacial friction factor similar to the one that contains Equations (2)–(12) which may be seen as improvements of models utilised earlier by Henstock & Hanratty (1976). The Reynolds Number of the liquid film (Re_{Lf}) was expressed by $Re_{Lf} = 4Q/P\nu_L$ with Q being the liquid film volumetric flow rate presumably evaluated with knowledge of the liquid film velocity. It is noteworthy that Equation (21) does not take into account entrainment into the gas core at high gas flow rates and deposition.

Work done by Hori et. al. (1978) to model film thickness in vertical upflow included the effect of the gas. They developed a correlation (Equation 22) which Fukano & Furukawa (1998) observed gives rather poor estimations at small values of δ/D_t.

$$\delta/D_t = 0.905Re_{GO}^{-1.45}Re_{LO}^{0.90}Fr_{GO}^{0.93}Fr_{LO}^{-0.68}(\mu_L/\mu_w)^{1.06} \quad (22)$$

Where:

$Fr_{LO} \equiv u_{sl}/\sqrt{gD_t}$, $Re_{GO} \equiv \rho_g u_{sg} D_t/\mu_g$.

μ_w and μ_L respectively, indicate the water viscosity at 20ºC and at conditions of experimental work.

Fukano & Furukawa (1998) obtained liquid film thickness and entrainment data from the work of Nishikawa et. al. (1967). This was tested using the Asali et. al.'s and Kosky's correlations and a good fit was achieved (

Figure **1**). The claim verifies that Nishikawa et. al.'s film thickness data is useful.

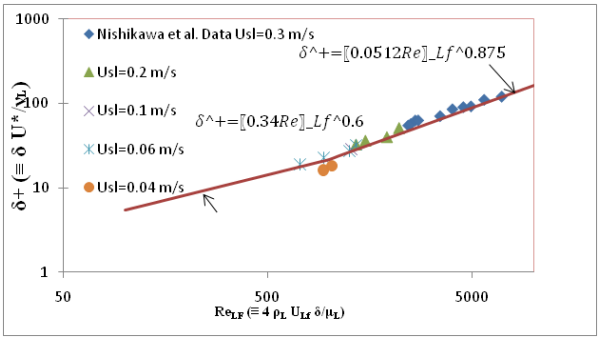

Figure 1: Prediction of Mean Liquid Film Thickness Using Data Reported By Nishikawa et al., (1967) for I.D= 25.1 mm

Fukano & Furukawa then developed a relationship that estimates the film thickness claiming it to be within 15% of the data. They used mixtures of air–water and air–glycerine to perform their experiment. This relationship is:

$$\delta/D_t = 0.0594\, exp(-0.34\, Fr_g^{0.25} Re_{Lf}^{0.19} x^{0.6}) \qquad (23)$$

The gas quality (x) is defined by the ratio of the gas mass flow rate to the total mass flow rates of liquid and gas, Fr_g is the Froude number of gas phase which can be obtained from the following equation:

$$\mathrm{Fr}_g = \frac{U_{sg}}{(gD)^{0.5}} \qquad (24)$$

Where:

g = 9.81 m/s^2 and U_{sg} is the superficial velocity of the gas phase and here the Reynolds number of the liquid film is expressed by:

$$Re_{Lf} = \frac{U_{Lf}\, D_t}{\nu_L} \qquad (25)$$

Where:

U_{Lf} and ν_L are the measured film velocity and the kinematic viscosity of liquid (m^2/s), respectively. They predicted the frictional pressure drop and the interfacial friction factor from the liquid film thickness. They revealed that their method estimates the liquid film thickness from a different point of view from other authors (e.g. Hewitt & Hall Taylor, 1970; Kosky, 1971; Henstock & Hanratty, 1976; Asali et al, 1985; Hewitt & Govan, 1990; and Ambrosini et. al., 1991) in that the procedure presented a pure correlation but is not iterative.

2 Description of Experimental Apparatus

The test facility illustrated in Figure 2 is specially structured to achieve the purpose of this study. The working fluids (namely, water and air) are supplied by a variable pump and Delta V system, respectively. The equipment consists of four tubes having a 4" internal diameter which is arranged in a vertical orientation and connected by U and inverted U-shaped bends. First, the gas phase enters the upward section through a T-shaped valve, while the water phase is pumped from the storage tank into the bottom section of the facility via a variable-speed pump. The gas and liquid are mixed together in the upward section and are flowing through the top bend before being initiated into the downward section of the pipe. Then they are flowing through the bottom bend to eventually reach the ventilation tank for separation. The conductance liquid film probes were installed at the upward and downward vertical legs of the pipe in order to extract the desired data.

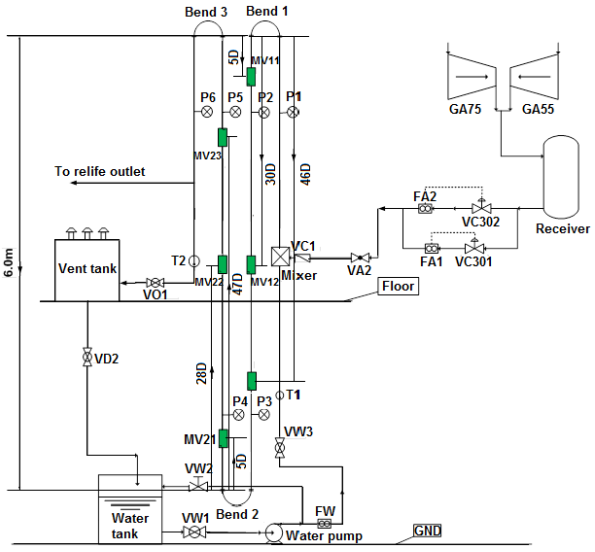

Figure 2: The Test Facility

3 Principles of Conductive Liquid Film Probes

In this study, four liquid film probes were installed on a probe spool, as presented in Figure 3. The spool comprises four sensors of film conductivity spaced 90 degrees from each other and mounted on the upward and downward pipes. The aim of this arrangement is to extract the circumferential distribution of the film thickness at the axial position of the vertical pipe.

For accurate results, the film thickness was periodically calibrated using acrylic blocks of various diameters concentrically inserted inside the film probe to generate a known thickness of the liquid layer. In order to gain precise measurements, the temperature variations were also considered, which were corrected for different ranges starting from 10 to 26˚C. Furthermore, measurement repeatability was performed to determine the possible uncertainty. It was found from the test of reliability that the recorded uncertainty was around 0.1 mm, which may give an error of ±3.3%.

Figure 3: The Conductance Liquid Film Probes

4 Experimental Data

Film thickness and film velocity data were collected at superficial velocities of liquid equal to 0.1, 0.2, 0.3, 0.48 & 1.0 m/s. These are presented in Table 1

Table 1: Film Thickness, Film and Fluid Velocities Collected for the Present Work

u_{sl} (m/s)	u_{sg} (m/s)	u_{Lf} (m/s)	δ (mm)
0.10	18.40	0.86	1.08
0.10	24.10	1.22	0.93
0.10	29.35	1.36	0.66
0.20	17.32	1.02	1.11
0.20	22.41	1.30	1.03
0.20	26.87	1.26	0.99
0.30	16.88	1.07	1.07
0.30	21.41	1.31	1.04
0.30	25.63	1.33	0.99
0.48	15.77	1.33	1.09
0.48	19.82	1.36	1.14
0.48	23.39	1.40	1.15
1.00	9.85	0.50	1.45
1.00	13.53	1.02	1.33
1.00	16.56	1.44	1.24
1.00	19.24	1.40	1.07

4.1 Trend of Mean Film Thickness with Superficial Fluid Velocities

The overall tendency for air–water upward flow is for the average film thickness to decrease with increasing the gas velocity into higher values. This is in good agreement with the results of liquid film thickness obtained here, as shown in Figure4. It can be seen from Figure 4 that the liquid film thickness values are decreased as the points of constant superficial liquid velocities become smaller.

Fukano & Furukawa (1998) and MacGillivary & Gabriel (2003) made similar observations reporting that average liquid film thickness decreases asymptotically, not linearly, with the mass flux of gas phase (by extension superficial velocity of gas) to minimum values regardless of liquid velocity. Ariyadasa (2002) attributed this asymptotic reduction to the fact that the liquid film becomes smoother when the gas velocity increases to higher values.

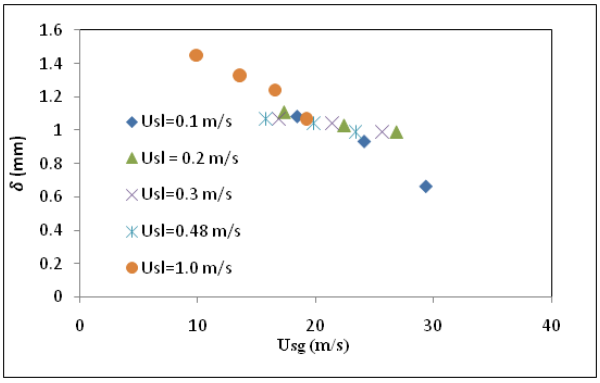

Figure 4: Variations of Mean Liquid Film Thickness with Superficial Gas Velocities

4.2 Comparison of Experimental Data with the Models Available in the Literature

Henstock & Hanratty's (1976) model (Equation 21) was used to obtain the dimensionless liquid film thickness (δ/D_t) when the Reynolds number of the liquid film expressed by $Re_{Lf} = 4\rho_L U_{Lf}\delta/\mu_L$. The trend of the obtained dimensionless film thickness generally follows that of the measured values but point-to-point prediction may not be considered to be in complete agreement (Figure). The dissimilarity may be due to the fact the model was derived without giving consideration to droplet entrainment due to high gas velocities. However, as can be seen, most of the predictions are within 20% of the measured experimental values.

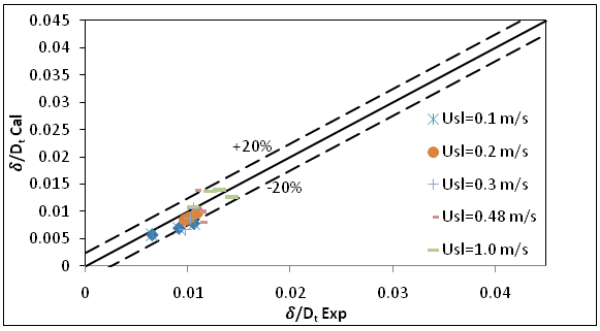

Figure 5: Comparison of the Dimensionless Film Thickness (Obtained from the Current Study) and Model Reported by Henstock & Hanratty (1976)

Similarly, Figure 6 illustrates respectively, a comparison of experimental δ/D_t and that estimated by Fukano & Furukawa's (1998) correlation (Equation 22). It is noted that only the predictions for superficial gas velocities of at least 24 m/s are generally consistent with the experimental results achieved from this work.

Figure 6 presents that the correlation's predictions at high gas (and low liquid) superficial velocities are within 15% of this work's experimental δ/D_t.

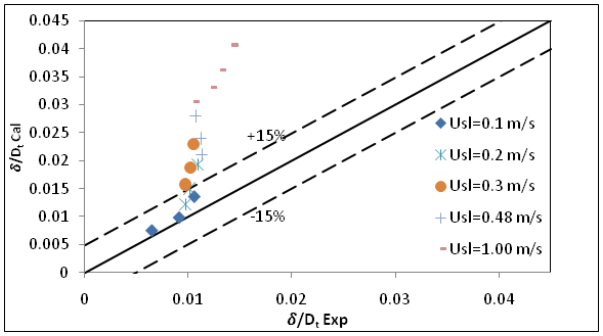

Figure 6: Comparison of Experimental Dimensionless Film Thickness with Values Extracted from the Model of Fukano & Furukawa (1998)

On the other hand, significantly poor predictions were obtained for thicker films at low u_{sg} values. The large discrepancy may be attributed to the fact that Fukano & Furukawa performed their results using a small internal diameter pipe (i.e., equal to 26 mm). As such, their model does not accurately consider the thick films in channels with diameters excess of 100 mm such as the pipe used for this work which has a diameter of 101.6 mm.

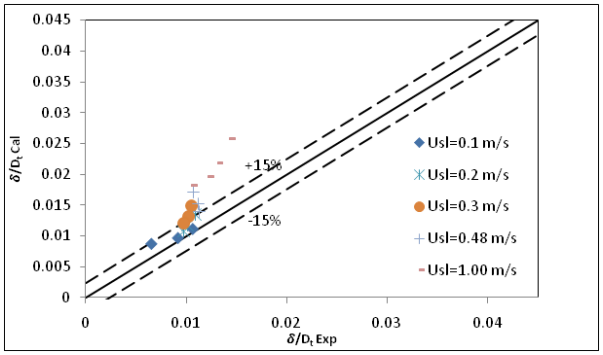

Figure 7: Comparison of Experimental Film Thickness with Values Extracted from the Model of Hori et al. (1978)

Figure 7 above shows the comparison of the current experimental study of liquid film thickness with values extracted from the Model of Hori et. al. (1978). It was noted that the predictions at high gas and liquid superficial velocities ranging from 0.1 to 0.3 m/s are within 15% of this work's experimental δ/D_t. For the other liquid velocities, pore prediction was noted which exceeds 15 %.

Figure 8 compares the predictions of the three models surveyed with the experimental data. Hori et al.'s (1978) and Henstock & Hanratty's (1976) models performed better than Fukano & Furukawa's over the range of u_{sg} values. This is also attributed to the strong exponential dependence of liquid film thickness for large ranges of u_{sg}, as described by Fukano & Furukawa's model.

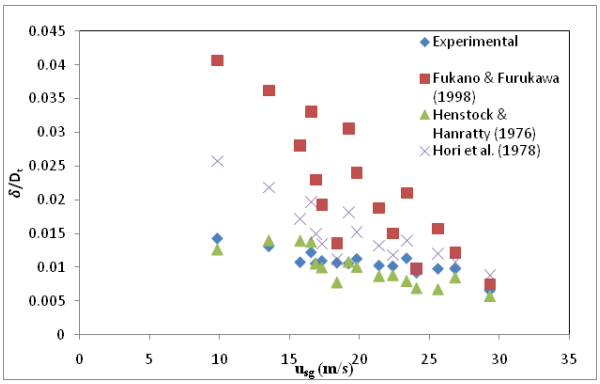

Figure 8: Variations of the Three Models' Dimensionless Film Thickness With Superficial Gas Velocities

Figure 9 shows how the data obtained for this work compares against Kosky's (1971) equation which is Equation 1. As can be seen, the fit is approximate with a lot of scatters on both sides of the line. The scatter may be attributed to the fact that in calculating Re_{Lf} using our data, liquid entrainment and deposition were not considered. The assumption that equilibrium flow occurs in the pipe can be made in that at high u_{sg} values, droplets were entrained into the core of the gas phase and are rapidly deposited. Hewitt & Govan (1990) pointed out that this assumption of equilibrium can only be made where adiabatic flow is concerned where there is zero heat transfer. However, where heat transfer between the phases is concerned in the so-called diabetic flows (e.g. flows with condensation or evaporation), there are considerable departures from equilibrium and the assumption collapses. In this work, heat transfer was not present and the flow can be classed as equilibrium. Thus, it is envisaged that the discrepancy between the rates of entrainment and deposition will be negligible leading to very little if any improvement in the fit. The scatter may also have occurred due to the difference in pipe diameter between the data used in developing the model (small, <100 mm) and this work's (large, 101.6 mm).

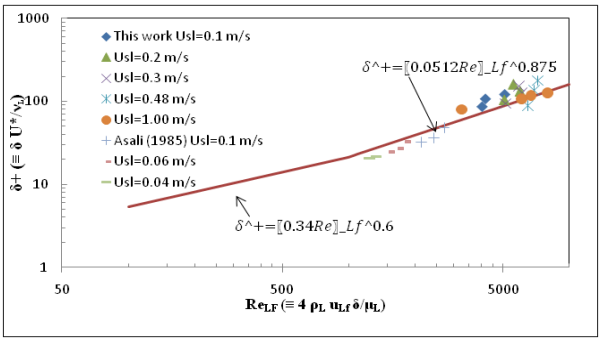

Figure 9: Mean Liquid Film Thickness Prediction Using Kosky's (1971) Model With This Work's Data and Asali's (1985) Entrainment Data

Asali et. al. (1985) entrainment data (using D_t=22.9 mm) did not fare much better against Kosky's correlation either (developed using D_t=42 mm with taken into consideration the possibility of entrainment), as can be seen from
Figure . This then lends credence to the suspicion that the tube diameter impact is considerable and there is a need for the modified equations to cater for large-sized channels in vertical gas-liquid upflow.

Table 2: A Summary of Experimental Conditions Used by Some of the Reviewed Literature for Air/Water Upflow in Vertical Pipes

No..	Source	Pipe Diameter (mm)	Axial distance to Sensor ($\times D_t$)	Range of u_{sg} (m/s)	Range of u_{sl} (m/s)
1	Asali et al (1985)	23, 42	n/a	n/a	n/a
2	Ambrosini et al (1991)	10–42.2	n/a	>25 m/s	0.012 – 0.7
3	Kaji & Azzopardi (2010)	19	300	0.87 – 33.9	0.03 – 0.65
4	Fukano & Furukawa (1998)	19.2, 26	n/a	10–50	0.04–0.3
5	Hewitt & Govan (1990)	7.72	n/a	n/a	n/a
6	Holt et al (1999)	5–10	180	3.67 – 67	0.04 – 0.14
7	Henstock & Hanratty (1976)	25.4	200 - 550	10 - 100	0.015 – 0.7
8	Omebere-Iyari et al. (2008)	5	400	0.06 – 50	0.03 – 0.65

4.3 Comparisons of the Current Study Against Empirical Models and Previous Experimental Work

Most of the available studies are focused on small-sized pipes. However, the structure of the liquid film in large pipe diameters is substantially different. However, several empirical models reported that the liquid film structure is directly affected by the pipe diameter and its orientation. Investigation of liquid film behavior in large-sized pipes is still very rare. Therefore, this study deals with the effects of large-diameter pipes on the liquid film characteristics. Comparisons of the current study with available imperial methods were presented in the subsections to reveal the applicability of these models in small and large pipes.

4.4 Comparison of the Current Study With That Reported by Webb and Hewitt (1975)

Webb and Hewitt (1975) conducted their experimental work in two small diameter pipes (i.e., having internal diameters of 31.8 & 38.2 mm) in a vertically downward direction. It was noted that the annular flow obtained in this study (with i.d= 101.6 mm) needs higher flow rates than that obtained by Webb and Hewitt (1975) where the diameter was relatively small. It can be concluded that for large-diameter pipes, higher flow rates are required to establish an annular flow than the smaller-diameter pipes. Hence, for a given flow rate, the region of any flow regime in large pipes is considerably different than that in small pipes, as illustrated in Figure 10.

Figure 10 presented the results of liquid film thickness conducted in large and small diameter pipes (namely, this study and experimental data reported by Webb and Hewitt (1975)). The data on liquid film thickness were performed using Henstock and Hanratty's (1976) model which is also illustrated in Figure 10. The model is considered the gas and liquid Reynolds number, as expressed in the following equation:

$$\frac{\delta}{D} = \frac{6.59\,F}{(1+1400\,F)^{\frac{1}{2}}} \tag{26}$$

$$F = \gamma\left(\frac{\vartheta_L}{\vartheta_G}\right)\left(\frac{\rho_L}{\rho_G}\right)^{\frac{1}{2}} Re_G^{-0.9} \tag{27}$$

$$\gamma = [(0.707\,Re_L^{0.5})^{2.5} + (0.0379 Re_L^{0.9})^{2.5}]^{0.4} \tag{28}$$

Where $D, \gamma, \vartheta_L \& \vartheta_G$ are respectively, the diameter pipe, film thickness, and kinematic viscosities of liquid and gas. The Reynolds numbers Re_G and Re_L for small-sized pipes are based on the gas and liquid flow rates.

It can be seen that the correlation presented a good agreement of the liquid film results when the small pipe data were used, while over-prediction was noted when it was applied to the large pipe (this study). The results of the falling film are achieved using the correlation reported by Karapantsios et al. (1989) and illustrated in Figure 10.

$$\delta = \left(\frac{\vartheta^2}{g}\right)^{\frac{1}{3}} Re^{0.538} \tag{29}$$

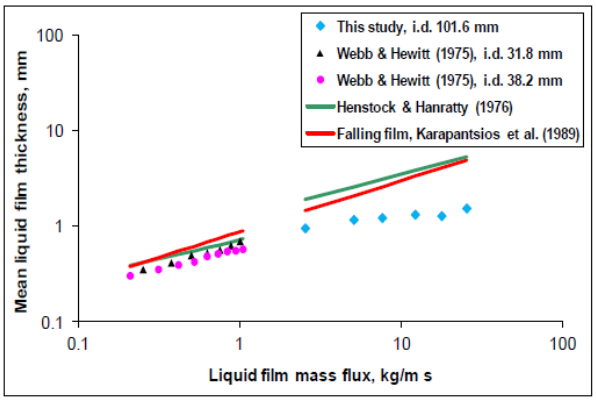

Figure 10: Liquid Film Behavior in the Region of Downward Annular Flow for Gas Velocity =9 m/s. Note: The Data of This Study Were Obtained at 30 Pipe Diameter After the Higher Bend, and at 19 Pipe Diameter After the Inlet Point for the Small Pipes

4.5 Modified Models of Henstock & Hanratty (1976) and Karapantsios et al. (1989)

Substantial discrepancies were observed for the larger pipe diameter (this study) when the models of Henstock & Hanratty (1976) and Karapantsios et al. (1989) were applied. However, these correlations gave a reasonable estimation for the data of Webb & Hewitt (1975) where the small pipe diameter was used. Therefore, it was necessary to modify these empirical correlations to be applicable to both pipe sizes. The modifications were performed based on changing their constants, as shown below:

$$\frac{\delta}{D} = \frac{6.5\,F}{(1+1400\,F)^{0.75}} \tag{30}$$

$$\delta = \left(\frac{\vartheta^2}{g}\right)^{\frac{1}{3}} Re^{0.41} \tag{31}$$

Figure 11 illustrates the structure of the liquid film in this study using the modified models of Henstock & Hanratty (1976) and Karapantsios et al. (1989) for gas velocity=9 m/s. It was worth mentioning that the data of this study were obtained at 30 pipe diameter after

the higher bend, and at 19 pipe diameter after the inlet point for the small pipes. It can be seen from Figure 11 that the new correlations presented a closer estimation of mean liquid film thickness when they are compared with the data of the large-sized pipe (the current study).

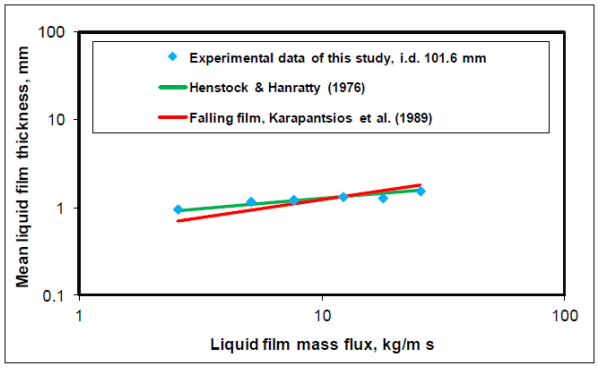

Figure 11: Liquid Film Behavior in the Current Experimental Work Using the Modified Models of Henstock & Hanratty (1976) and Karapantsios et al. (1989) For Gas Velocity=9 m/s. Note: The Data of This Study Were Obtained at 30 Pipe Diameter After the Higher Bend and at19 Pipe Diameter After the Inlet Point for the Small Pipes

Figure 12 shows the modified models reported by Henstock & Hanratty (1976) and Karapantsios et al. (1989) for small and large pipe diameters. The modified correlations were respectively, for Henstock & Hanratty (1976) and Karapantsios et al. (1989), as illustrated in the following correlations:

$$\frac{\delta}{D} = \frac{7.1\,F}{(1+1400\,F)^{0.73}} \tag{32}$$

$$\delta = 0.45\,(\frac{\vartheta^2}{g})^{\frac{1}{3}}\,Re^{0.45} \tag{33}$$

Figure 12, clearly shows that the modified models (32) & (33) presented a good estimation when applied for this study and the experimental data reported by Webb & Hewitt (1975). The results extracted from the present work and Webb & Hewitt (1975) gave very close predictions to each other. In both studies, the liquid film is increased with increasing the mass flux of the liquid phase. This was attributed to the fact that the liquid film is thicker for the higher water velocities. It can be seen from Figure 12 that the modified models can be used for large and small sized pipes.

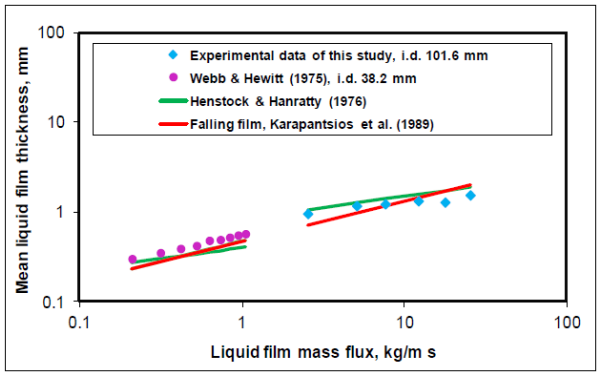

Figure 12: Liquid Film Behavior in the Current Experimental Work and That Reported by Webb & Hewitt (1975) Using the Modified Models of Henstock & Hanratty (1976) and Karapantsios et al. (1989) For Gas Velocity=9 m/s. Note: The Data of This Study Were Obtained at 30 Pipe Diameter After the Higher Bend and at19 Pipe Diameter After the Inlet Point for the Small Pipes

5 Conclusions

1- It was noted from this study that the empirical model of Henstock and Hanratty (1976) presented a good agreement when applied for small pipe diameter (i.e., for internal diameter= 31.8 mm), but it overestimated the experimental data of liquid film obtained from the current study (i.e., for internal diameter= 101.6 mm).

2- It was found from the analyzed data that the falling film presented the highest values when compared with data from Webb and Hewitt (1975). This was attributed to the fact that the falling liquid film in concurrent gas states is thinner than that without concurrent gas states.

3- It was also found that the analyzed data of the current work are higher when the correlation of Henstock and Hanratty's (1976) was applied. Laurinat et. al. (1984) stated that the over- prediction of the liquid film thickness was due to the fact that the model of Henstock and Hanratty (1976) neglected the entrainment droplets into the pipe centre for the downflows when the highest region of the annular flow is considered. It was worth mentioning that the liquid film Reynolds number is expressed in the following formula:

$$Re_{LF} = \frac{\tau}{\mu} \tag{34}$$

According to Dukler and Bergelin (1952), the range of Reynolds numbers starting from 200 to 1000, will lead to the generation of a wavy flow pattern having disturbance waves. These waves are accompanied by

liquid entrainment into the pipe centre and may have occurred on the liquid film surface as a result.

4- Finally, it can be concluded that the modified models gave a very good prediction when applied to this study and those reported by Webb & Hewitt (1975). In the meantime, the results extracted from the present work and experimental work of Webb & Hewitt (1975) are consistent and give very close predictions to each other. In both studies, the liquid film was increased with increasing the mass flux of the liquid phase. This was attributed to the fact that the liquid film is thicker for the higher water velocities. Therefore, the modified models can be used for large and small-sized pipes.

References

Ambrosini, W., Andreussi, P & Azzopardi, B J, (1991). A physically based correlation for drop size in annular flow. *International Journal of Multiphase Flow*, 17(4), pp.497–507.

Ariyadasa, U. (2002). An investigation of film thickness and pressure in upward and downward annular two-phase flow. M.Sc. thesis, Department of Mechanical Engineering, University of Saskatchewan.

Asali, J.C., Hanratty, T J & Andreussi, Paolo, (1985). Interfacial drag and film height for vertical annular flow. *AIChE Journal*, 31(6), pp.895–902.

Dukler, A. E., Bergelin, O. P. (1952). Characteristics of flow in falling films. *Chemical Engineering Progress*, 48, pp. 557-563.

Fukano, T. & Furukawa, T., (1998). Prediction of the effects of liquid viscosity on interfacial shear stress and frictional pressure drop in vertical upward gas-liquid annular flow. *International Journal of Multiphase Flow*, 24(4), pp.587–603.

Henstock, W.H. & Hanratty, Thomas J, (1976). The interfacial drag and the height of the wall layer in annular flows. *AIChE Journal*, 22(6), pp.990–1000.

Hewitt, G.F. & Govan, A.H., (1990). Phenomenological modelling of non-equilibrium flows with phase change. *International Journal of Heat and Mass Transfer*, 33(2), pp.229–242.

Hewitt, G.F. & Hall-Taylor, N.S., (1970). *Annular two-phase flow,*, Oxford; New York: Pergamon Press.

Hori, K. et al., (1978). Study of ripple region in annular two-phase flow (Third report, effect of liquid viscosity on gas-liquid interfacial character and friction factor). *Trans. Jap. Soc. Mech. Eng.*, 44(387), pp.3847–3856.

Kaji, R. & Azzopardi, B.J., (2010). The effect of pipe diameter on the structure of gas/liquid flow in vertical pipes. *International Journal of Multiphase Flow*, 36(4), pp.303–313.

Kelessidis, V. C. and Dukler, A. (1989). Modelling flow pattern transitions for upward gas-liquid flow in the vertical concentric and eccentric annulus. *International Journal of Multiphase Flow*, 15, pp.173-191.

Kosky, P.G., (1971). Thin liquid films under simultaneous shear and gravity forces. *International Journal of Heat and Mass Transfer*, 14(8), pp.1220–1224.

Laurinat, J. E., Hanratty, T. J. and Dallman, J. C. (1984). Pressure drop and film height measurements for annular gas-liquid flow. *International Journal of Multiphase Flow*, 10, pp. 341-356.

MacGillivary, R.M. & Gabriel, K.S., (2003). A study of annular flow film characteristics in microgravity and hypergravity conditions. *Acta Astronautica*, 53(4–10), pp.289–297.